

Full length article

Hot-isostatic-pressed Cr:ZnSe ultrafast laser at 2.4 μm Yuchen Wang^a, Fiona Fleming^b, Richard A. McCracken^b, Carl Liebig^c, Sean McDaniel^c, Gary Cook^c, Paolo Laporta^{a,d}, Ajoy K. Kar^b, Gianluca Galzerano^{a,*}^a Istituto di Fotonica e Nanotecnologie - Consiglio Nazionale delle Ricerche, Piazza L. Da Vinci, 32, Milano 20133, Italy^b Institute of Photonics and Quantum Sciences, Heriot-Watt University, Edinburgh EH14 4AS, Scotland, UK^c Sensors Directorate, Wright-Patterson Air Force Base, 2241 Avionics Circle Bldg. 620, Dayton 45433, Ohio, USA^d Dipartimento di Fisica - Politecnico di Milano, Piazza L. Da Vinci, 32, Milano 20133, Italy

ARTICLE INFO

Keywords:

Ultrafast mid-infrared laser
Kerr-lens mode-locked laser
Transition metal doped crystal
Mid-infrared laser crystal

ABSTRACT

We report on a room temperature Kerr-lens mode-locked chromium-doped zinc selenide (Cr:ZnSe) laser emitting four optical-cycles pulses in the mid-infrared spectral region in which the laser polycrystal has been treated by hot isostatic pressing (HIP). The laser emits 34 fs pulses at 2.4 μm , with a repetition rate of 171 MHz and average output power capabilities of up to 150 mW. This is the first mode-locking investigation conducted using the HIP treated material and to our knowledge, is the shortest pulse width demonstrated, to date, from polycrystalline Cr:ZnSe. The experimental comparison with respect to an untreated polycrystal indicates that HIP treatment is advantageous for mode-locking action of this active material.

1. Introduction

Transition metal doped II-VI semiconductors (TM:II-VIs) were initially introduced as active gain media in the mid-1990s [1], and since then they have become arguably the favored emission sources in the mid-infrared (2–5 μm) spectral region [2]. This is because they allow for directly stimulated emission at wavelengths spanning 1.8–6 μm , in the form of a compact and robust solid-state laser source. The capability of these sources to operate in an ultrafast mode-locked regime emitting few-optical-cycle pulses is very important for a variety of applications, including, for example precise material processing [3], and medical diagnostics, such as human breath analysis using ultra-broadband spectroscopy [4]. Moreover, these ultrafast mid-IR sources are vital for wide-span, high powered frequency combs for high precision spectroscopy, metrology and imaging in the molecular fingerprint region from 2.5 to 20 μm [5]. Recently, particular attention has been focused on the development of ultrafast Cr:ZnS and Cr:ZnSe lasers at 2–3 μm , where many gas molecules exhibit strong characteristic absorption features [6,7]. Cr:ZnS and Cr:ZnSe have a broad emission cross section, characteristic of TM:II-VI, spanning 1.8 to 3.2 μm and 1.9 to 3.3 μm ranges, respectively [2]. Consequently, extensive development has led to the achievement of highly efficient room temperature CW performance with output power capabilities reaching several tens of watts [8,9], and sub-100 fs pulses in the pulsed regime [7,10–18]. Thus, they have become an

attractive replacement for the complex, bulky optical parametric oscillators (OPOs) based on down conversion of a near IR laser sources, which previously dominated the field of ultrafast pulse generation in this spectral region. With specific attention to polycrystalline Cr:ZnSe, the first demonstration of mode-locking was achieved in 2000 with the use of an acousto-optic modulator (AOM). This laser demonstrated 4.4 ps pulses at a pulse repetition frequency (PRF) of 82 MHz, with average output power of 82 mW [19]. The development of semiconductor saturable absorber mirrors (SESAMs) for use in the mid-IR used in combination with a prism pair and chirped mirrors, respectively, for group delay dispersion (GDD) compensation, allowed for dramatic reduction in pulse duration to ~ 100 fs [20] and ~ 80 fs [10]. A graphene based saturable absorber with a prism pair has generated 226 fs pulses, [21], but the remarkable operational bandwidth of graphene indicates that this could be further shortened. The high intracavity powers required to power-scale these resonators often results in damage to the graphene [6] limiting their output power to tens of mW. The technique of Kerr-lens mode-locking (KLM), which exploits the nonlinear self-focusing effect in the active laser material to realize a virtual fast saturable absorber, is an effective method to obtain ultra-short pulses. In the highly nonlinear Cr:ZnSe crystal, KLM has resulted in remarkable improvements in the laser performance as the issue of potential damage to a physical saturable absorber has been eliminated. This mechanism has enabled the generation of pulses with 38 – 47 fs durations [13–16],

* Corresponding author.

E-mail address: gianluca.galzerano@polimi.it (G. Galzerano).

which, to the authors knowledge are the shortest pulse durations demonstrated with Cr:ZnSe prior to this report. An even shorter pulse duration of 23 fs, corresponding to 3-optical cycles, has been demonstrated in the same spectral region at around $2.4 \mu\text{m}$ by KLM of polycrystalline Cr:ZnS laser [18].

In this paper we report, for the first time, the KLM of hot isostatic pressing (HIP)-treated polycrystalline Cr:ZnSe. The laser demonstrated the shortest pulse duration at $2.4 \mu\text{m}$ ever obtained with Cr:ZnSe active medium, 34 fs covering a spectral bandwidth, full width at half maximum (FWHM), of $\sim 200 \text{ nm}$, indicating that HIP treatment is advantageous not only for the CW laser emission but also for mode-locking of this polycrystal. Up to now, the use of HIP-treated polycrystalline Cr:ZnSe materials has been demonstrated only in CW laser action as reported by Stites et al. [22], where they presented results of utilizing HIP for the diffusion process of transition metals into the host, and separately as a post-dopant treatment. In both cases the resultant CW laser spectral linewidth in a bulk resonator is reduced from $\sim 10\text{s}$ of nm to sub-nm levels. This effect has also been demonstrated in Fe:ZnSe [23]. The proposed reason for this spectral narrowing is that HIP converts inhomogeneously broadened material to homogeneously broadened material. HIP treatment causes this conversion by removing defect centers and to reducing the number of grain boundaries within the crystal. These lead to the strong inhomogeneous broadening exhibited in commercially available untreated polycrystalline Cr:ZnSe. Here by comparing the laser performance in both CW and KLM regimes of a polycrystalline Cr:ZnSe active medium before and after HIP treatment, we demonstrated that HIP treatment is beneficial not only for CW regime but also for mode-locking laser action. In particular, after HIP-treatment the KLM pulse duration shortened from 58 fs down to 34 fs, using the same experimental configuration exploited with the untreated Cr:ZnSe polycrystal.

2. Experimental setup

The active medium used in the laser experiments is a commercially available Cr:ZnSe polycrystal (IPG Photonics) with a dopant concen-

tration of $5.78 \times 10^{18} \text{ cm}^{-3}$ and dimensions $5 \times 6 \times 3 \text{ mm}$ (height \times width \times thickness). First, we performed both CW and KLM laser experiments with this untreated polycrystal. Then, the polycrystal was HIP treated and the same set of laser experiments were conducted to clearly investigate the effect of the HIP treatment. The HIP process is summarised as follows: the sample was sealed within a high pressure/temperature chamber, subsequently the temperature and pressure were raised over two hours to values of 1050°C and 30,000 PSI, respectively. Inert argon gas was used as a buffer for the isostatic process. The samples were held at these conditions for two hours before temperature reduction and gas ventilation over an additional two hours. A more detailed description of the process can be found in reference [22]. Fig. 1 (a) shows the scheme of the four-mirror linear resonator used for both CW and KLM laser experiments. The x-folded linear resonator consists of two curved chirped mirrors (CMs), 50-mm radius of curvature, one plane CM and a plane output coupler. The CMs are coated for high reflectivity ($> 99.5\%$) in the region $2.2\text{--}2.8 \mu\text{m}$ with an average group delay dispersion (GDD) of -300 fs^2 and for high transmissivity ($> 95\%$) in the pumping wavelength region from 1.5 to $2.0 \mu\text{m}$. The Cr:ZnSe polycrystal is secured on a copper heat sink which is held at a temperature of 20°C using a Peltier-electric cooler in which the heat is dissipated by water cooling. The pump source is a linearly polarized CW $1.94 \mu\text{m}$ wavelength Tm:fibre laser (IPG Photonics, TLR-LP-20) with maximum output power of 20 W. The sample is placed at Brewster's angle (68°) at the point of focus between the curved mirrors and the pump beam is focused into the crystal (calculated spot sizes $25 \times 29 \mu\text{m}^2$) through the curved CM with an AR-coated plano-convex lens of 40 mm focal length. The propagation length through the crystal is 3.24 mm and the single-pass absorption of pump light is $\sim 70\%$. The cavity folding angles are $\sim 18^\circ$ in both arms of the resonator to compensate for the astigmatism imposed by the Brewster-angled crystal surfaces. For CW laser experiments the x-folded cavity is configured with symmetric arm lengths of about 250 mm ($\sim 1:1$ ratio) and a separation of the curved mirrors of $\sim 51 \text{ mm}$, corresponding to the center of the resonator stability condition, see Fig. 1 (b), allowing for laser mode beam dimensions in the center of the laser polycrystal of $28 \times 32 \mu\text{m}^2$. In KLM the arrangement of the resonator is

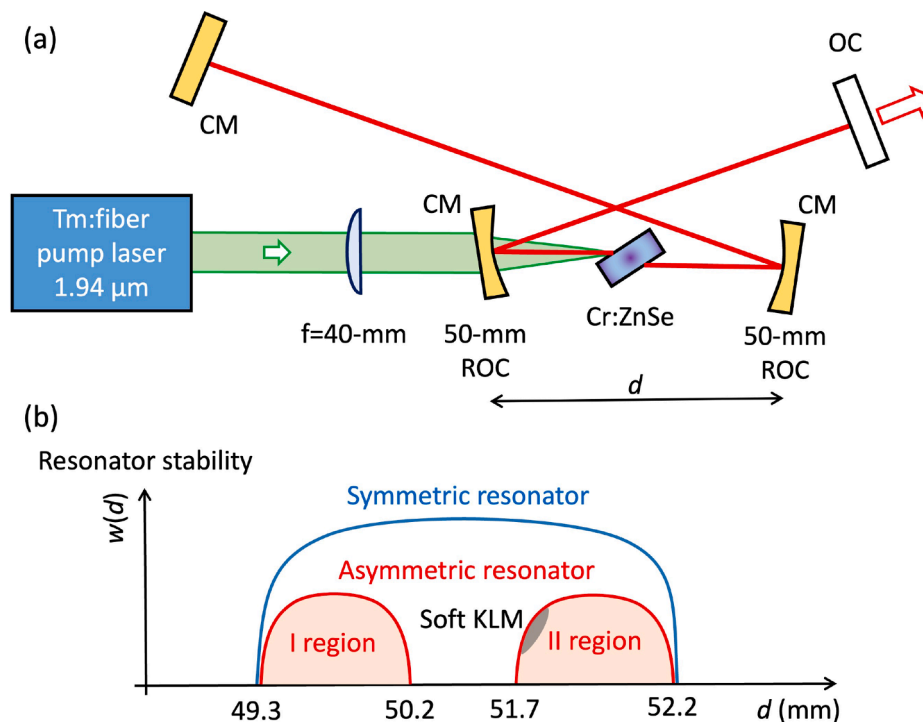


Fig. 1. (a) Laser resonator for CW and KLM laser experiments. CM: chirped mirror; OC: output coupler. (b) Stability condition versus the separation between the curved CMs, d , for symmetric and asymmetric cavity configuration, where $w(d)$ is the laser spot size in the Cr:ZnSe polycrystal.

asymmetric with the ratio of the arm lengths $\sim 5:6$ and the total length of the cavity equal to 88 cm. The separation between the curved mirrors is in the range from 51.7 to 52.2 mm, corresponding to the second stability zone of the resonator where soft-aperturing KLM is obtained [24], as sketched in Fig. 1 (b). The group velocity dispersion (GVD) of ZnSe at 2.4 μm is $+209 \text{ fs}^2\text{mm}^{-1}$, resulting in GDD of $+1354 \text{ fs}^2$ (round trip). Data provided by the chirped mirror suppliers give a GDD value of $-300 \pm 30 \text{ fs}^2$ per bounce at the 2.4- μm laser wavelength and thus the total GDD due to the chirped mirrors is: $-300 \text{ fs}^2 \times 5 = -1500 \pm 70 \text{ fs}^2$. The GDD of the atmosphere and the unknown value of the output coupler are assumed negligible in this estimation. This results in a calculated net round-trip cavity GDD value of $-146 \pm 70 \text{ fs}^2$, therefore in the anomalous dispersion regime allowing for a quasi-soliton mode-locking operation.

3. Results

Fig. 2 (a) shows the output power as a function of the incident pump power when the laser operates in CW with the untreated (open circles) and HIP-treated polycrystal (open squares) for different output coupler values. It is worth noting that the HIP-treated case results in an overall improvement of the CW laser performance for all the exploited output coupling. In particular, for 20% output coupling the slope efficiency increases from 16% to 20% when the Cr:ZnSe polycrystal is HIP treated, allowing for a maximum output power of 610 mW (at incident pump power of 3.5 W). Furthermore, by comparing the threshold pump powers it is also evident that the HIP treatment does not introduce additional losses in the polycrystal. After CW laser characterization, the symmetric x-folded resonator is modified into the asymmetric configuration, as described in the previous section. Subsequently, the separation of the curved mirror, d , and the position of the crystal were finely adjusted by use of compact micrometer stages in order to identify the edges of the resonator stability regions where soft-aperture KLM can most likely be achieved. In this configuration, the CW laser efficiency was strongly reduced by more than 50%, as shown in Fig. 2 (b). KLM operation was initiated by sharp translation of the plane CM. It was found that KLM operation was not particularly difficult to start, and the

mode-locked emission was extremely stable over several hours. The mode-locked operation was verified by detection of the laser output with a 1 GHz extended InGaAs photodiode for the range 1.2–2.6 μm , (Hamamatsu, G8423-03SPL) connected to an oscilloscope. The average output power vs incident pump power characteristics in the KLM regime are shown in Fig. 2 (b) for both the untreated and HIP-treated polycrystal with 3% output coupling. KLM with the untreated polycrystal results in a slope efficiency of 4.2% and the mode-locking was found to start at a minimum pump power of 2.04 W. The maximum average output power measured was 140 mW for an incident pump power of 3.5 W, corresponding to an optical-to-optical efficiency of 6% with respect to the absorbed pump power. In the case of HIP-treated KLM the slope efficiency and mode-locking threshold are 4.0% and 2.05 W, respectively. The maximum average power was 158 mW measured at 3.5 W of pump power. It is worth noting that even in the case of the KLM regime the overall performance obtained with the HIP-treated polycrystal is slightly better than that demonstrated by the untreated polycrystal. In both cases, for pump power higher than 4 W the KLM becomes unstable, and the average output power decreases. This is likely due to thermal issues in the polycrystal; more efficient cooling may improve the stability for higher pump power levels.

At the maximum average power of 158 mW, the radio frequency spectrum of the KLM laser is shown in Fig. 3, in the case of HIP-treated polycrystal. Fig. 3 (a) shows the beat notes at the fundamental frequency of 171 MHz and its second harmonic, at 342 MHz, measured with a resolution bandwidth (RBW) of 1 MHz. A detailed measurement of the beat note at the fundamental frequency, with a higher RBW of 10 kHz, is shown in Fig. 3 (b). The high fundamental carrier signal-to-noise ratio (SNR), which is greater than 80 dB in the 10 kHz RBW, and the absence of any Q-switch sidebands in the RF spectrum prove the excellent pulse-to-pulse stability of the KLM regime. The same RF spectrum was observed also for the untreated polycrystal.

Regarding KLM pulse duration and spectral bandwidth, HIP-treatment produced, instead, significant improvements with respect to the un-treated case. Fig. 4 shows the spectral bandwidth and time duration of the KLM pulse trains obtained with HIP-treated and untreated polycrystal. The spectral output of the mode-locked pulses was

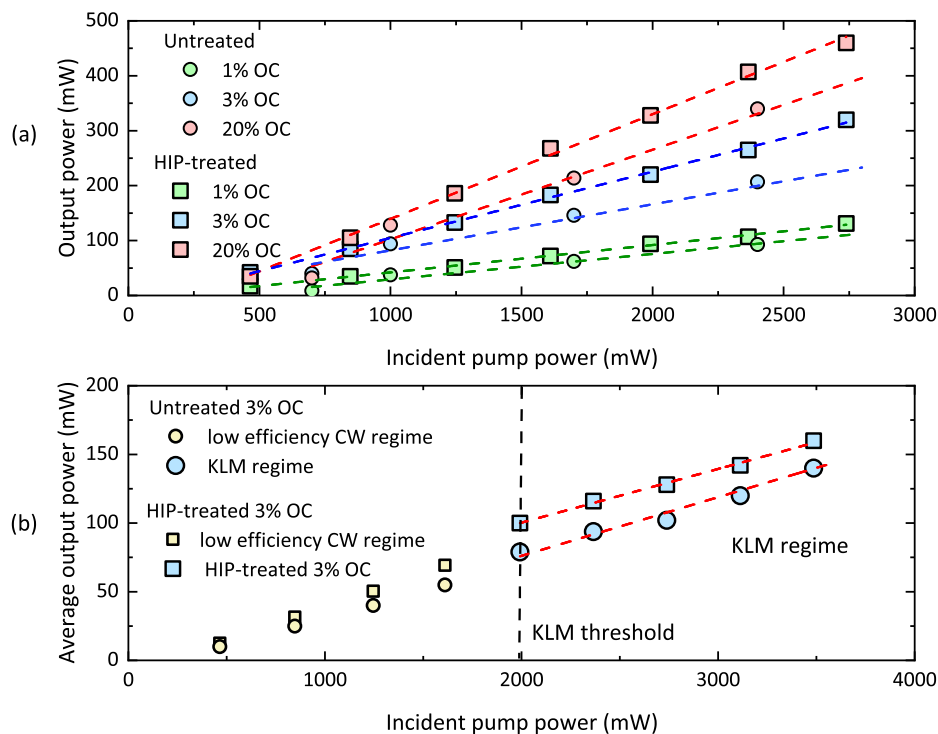


Fig. 2. Output power versus incident pump power in (a) CW and (b) KLM regimes for untreated (open circles) and HIP-treated (open squares) Cr:ZnSe polycrystal.

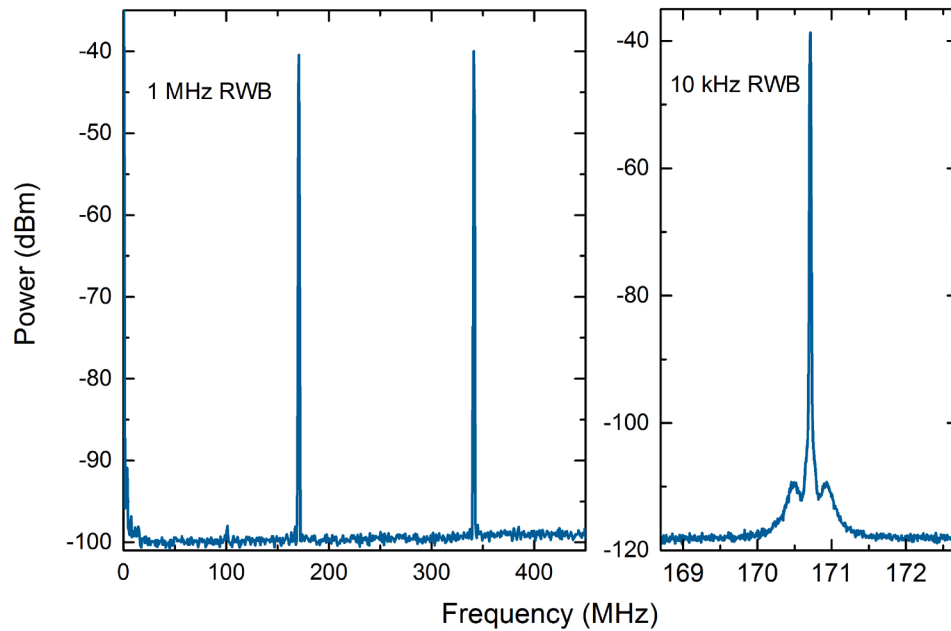


Fig. 3. Radio Frequency spectrum of mode-locked HIP-Cr:ZnSe laser. (a) Fundamental and second harmonic frequencies, measured over a span of 450 MHz and with a resolution bandwidth (RBW) of 1 MHz. (b) Detailed view of the beat note at the fundamental frequency over a 4 MHz span with a RBW of 10 kHz.

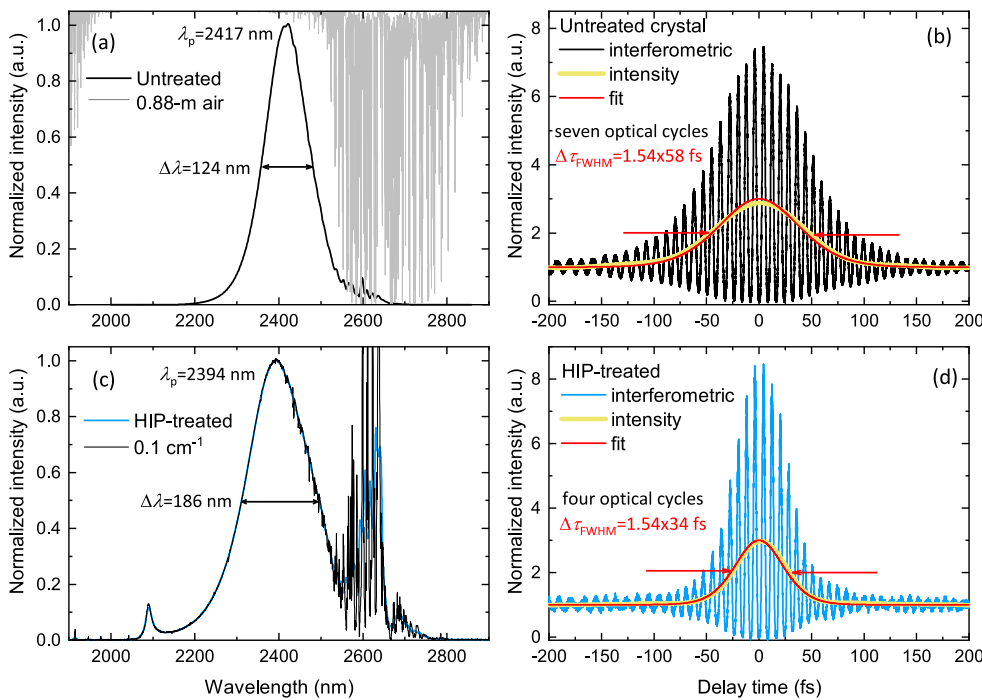


Fig. 4. KLM pulse train characterization with the 3% output coupler: (a) optical spectrum and (b) interferometric two-photon autocorrelation for untreated Cr:ZnSe polycrystal; (c) optical spectrum and (d) interferometric two-photon autocorrelation for HIP-treated Cr: ZnSe polycrystal. Yellow and red curves in panels (b) and (d) represent, respectively, the intensity autocorrelations obtained by numerically filtered interferometric autocorrelation traces and the fitting curves of intensity autocorrelation using hyperbolic secant pulse profile. Gray line in panel (a) represents the transmission of 0.88-m of standard air (HITRAN simulation [25]).

measured with a Fourier Transform infrared spectrometer operating in the 0.8–20 μm spectral region with a frequency resolution of 30 GHz (1 cm^{-1}), corresponding to a spectral bandwidth of ~ 0.6 nm). The temporal duration was characterized by an interferometric autocorrelation measurement. The autocorrelator employed a homemade set-up based on two-photon absorption in an InGaAs photodiode with a cutoff wavelength of 1.7 μm . In the case of untreated Cr:ZnSe KLM laser, reported in Fig. 4 (a), the spectral output is centered at 2417 nm with a FWHM of 124 nm. The corresponding interferometric autocorrelation trace in Fig. 4 (b) is characterized by the expected 8:1 peak-to-background ratio and a FWHM of 89 fs, which translates into a pulse

duration of 58 fs assuming a sech^2 pulse profile. The associated time-bandwidth product is therefore 0.368, slightly larger than the transform-limited value of 0.315 for sech^2 pulses. Figs. 4 (c) and (d) show, respectively, the spectral bandwidth and interferometric autocorrelation curves in the case of HIP-treated Cr:ZnSe laser. The spectral bandwidth, centered at 2395 nm, is broadened up to 187 nm FWHM, spanning from 2311 to 2498 nm (corresponding to a bandwidth of 9.7 THz). The interferometric autocorrelation trace, Fig. 4 (d), has a FWHM of 53 fs, which translates into a pulse duration of 34 fs assuming a sech^2 pulse profile, corresponding to four-optical cycles. The associated time-bandwidth product is 0.329, also in this case close to transform-limited

value. The quasi-soliton operation of our KLM laser is further supported by the appearance of the Kelly sideband at around $\sim 2.1 \mu\text{m}$ on the optical spectrum of the mode locked pulses, as shown in Fig. 4 (c). The Kelly sideband appeared mainly on one side of the optical spectrum, which suggests that the 2nd-order dispersion is well compensated in the laser, and the formed soliton pulse width is mainly determined by the 3rd-order dispersion of the cavity [26]. The features in the long tail of the spectra at around $2.6 \mu\text{m}$ reported in Figs. 4 (a) and (c) are due to the intracavity water absorption spectrum, due to the open resonator operating without a controlled atmosphere. This effect is more pronounced in the spectrum in Fig. 4 (c) due to the wider bandwidth obtained by the HIP-treated KLM laser that interacts with a greater number of water absorption lines. These spectral features, broadened by the FITR instrumental profile (1 cm^{-1}), are constituted by several narrow emission lines in coincidence with the maximum intracavity transmission windows. For comparison, Fig. 4 (c) reports also the same spectrum recorded with a resolution of 0.1 cm^{-1} (black curve) and the computed transmission spectrum for 0.88-m of standard atmosphere (gray curve), HITRAN database [25]. These spectral features at around $2.6 \mu\text{m}$ can be reduced operating the Cr:ZnSe laser in a pure nitrogen atmosphere to remove the water vapor absorption [18].

4. Discussion

These record results, in terms of pulse duration, indicate that HIP is advantageous for mode-locking polycrystalline Cr:ZnSe lasers. This benefit cannot be ascribed solely to the slightly increased KLM laser efficiency demonstrated by HIP-treated polycrystal, because the difference between intracavity pulse energies for un-treated and HIP-treated material (28 nJ and 31 nJ respectively, at 3.5 W pump power level), which is less than 10%, is far too low to justify the difference in pulse durations (58 fs versus 34 fs). Therefore, additional contributions related to the HIP-treatment need to be brought into play, and a possible explanation is that proposed by Stites et al. [22], concerning the transition from inhomogeneous to homogeneous broadening of the active material. In the former case, if the photon interaction time of propagating photons is less than the thermalization time, the energy cannot be redistributed across the gain spectrum at sufficient speed, resulting in the oscillating pulse burning a hole in the gain spectrum. This reduces the overall gain and leaves much of the excited state energy inaccessible to the building laser pulse. During the initiation of mode-locking whilst the pulse begins to form, if the pulse duration falls below that of the thermalization time the pulse compression process stalls, hence the duration is limited to the equivalent of the thermalization time. In polycrystalline solid state crystals such as ZnSe, where thermalization is determined through the phonon spectrum, this is of the order of ~ 100 s of fs [27], as a result the generation of few-cycle pulses can be difficult to achieve stably. The main challenge in the generation of ultrafast pulses from inhomogeneously broadened lasers is to lock the phases of all lasing longitudinal modes. When the mode-locking strength becomes weak and/or the GDD is large, the lockable bandwidth reduces. This instability due to the insufficient gain filtering is common and unique in inhomogeneously broadened lasers [28]. HIP treatment of polycrystalline material has two major effects: removal of crystalline defects and growth of the grains. Removal of defects means all ions experience the same crystal fields, thus the crystal acts as a homogeneously broadened material. In combination with defect removal, fewer grain boundaries reduce the phonon lifetime so even if the material is not perfectly homogeneously broadened the thermalization time is reduced in any residual inhomogeneously broadened fraction. Homogeneous broadening results in no spectral hole burning and the gain profile is uniformly depleted as the pulse builds. Any residual inhomogeneously broadened component has very small thermalization times, so the mode-locked pulse can still access the full gain spectrum. Net intracavity dispersion also has major consequences on resultant pulse duration. It is worth to note that the HIP-treatment does not introduce additional

crystal losses, as demonstrated by the CW laser experiments; moreover, we did not observe any significant improvement of the optical quality of the polycrystal after HIP-treatment, as verified by comparative scattering measurements at 650 nm . These results strongly suggest the laser is operating in a regime in which the thermalization time is less than the photon interaction time and as such has allowed for the generation of record short 34-fs pulse durations.

5. Conclusion

In conclusion, the HIP-treatment of Cr:ZnSe laser polycrystal has been investigated for Kerr-lens mode-locking for the first time. The experimental comparison of the laser performance obtained with the same laser polycrystal before the HIP-treatment demonstrated a substantial shortening of the pulse duration from 58 fs (untreated) to 34 fs (HIP-treated) and an increase of the mode-locking stability, thus indicating that HIP treatment is advantageous in the generation of ultrafast pulses in this polycrystal.

Funding

European Office of Aerospace Research and Development (FA8655-21-2-7001); UK Engineering and Physical Sciences Research Council (EP/G030227/1, EP/L504774/1, and EP/M506333/1).

Declaration of Competing Interest

The authors declare that they have no known competing financial interests or personal relationships that could have appeared to influence the work reported in this paper.

References

- [1] L.D. DeLoach, R.H. Page, G.D. Wilke, S.A. Payne, W.F. Krupke, Transition metal-doped zinc chalcogenides: Spectroscopy and laser demonstration of a new class of gain media, *IEEE J. Quantum Electron.* 23 (1996) 885–895.
- [2] S. Mirov, I. Moskalev, S. Vasilyev, V. Smolski, V. Fedorov, D. Martyshkin, J. Peppers, M. Mirov, A. Dergachev, V. Gapontsev, Frontiers of mid-ir lasers based on transition metal doped chalcogenides, *IEEE J. Sel. Top. Quantum Electron.* 24 (2018) 1–29.
- [3] A.H. Nejadmalayeri, P.R. Herman, J. Burghoff, M. Will, S. Nolte, A. Tunnermann, Inscription of optical waveguides in crystalline silicon by mid-infrared femtosecond laser pulses, *Opt. Lett.* 30 (2005) 964–966.
- [4] R. Steiner, Medical applications of mid-ir solid-state lasers, in: M. Ebrahimzadeh, I. T. Sorokina (Eds.), *Mid-Infrared Coherent Sources and Applications*, Springer, The Netherlands, 2008, pp. 575–588.
- [5] F.K. Tittel, D. Richter, A. Fried, Mid-infrared laser applications in spectroscopy, *Solid State Mid-Infrared Laser Sources*, I.T. Sorokina, K.L. Vodopyanov (Eds.) (Springer (2003) 458–592.
- [6] I.T. Sorokina, E. Sorokin, Femtosecond cr^{2+} -based lasers, *IEEE J. Sel. Top. Quantum Electron.* 21 (2015) 273–291.
- [7] S. Vasilyev, I. Moskalev, M. Mirov, V. Smolski, S. Mirov, V. Gapontsev, Ultrafast middle-ir lasers and amplifiers based on polycrystalline cr:zns and cr:znse, *Opt. Mater. Express* 7 (2017) 2636–2650.
- [8] S. Mirov, V. Fedorov, D. Martyshkin, I. Moskalev, M. Mirov, S. Vasilyev, High average power fe:znse and cr:znse mid-ir solid state lasers, *Advanced Solid-State Photonics*, OSA Technical Digest Series (CD) (Optical Society of America) (2015) AW4A.1.
- [9] I. Moskalev, S. Mirov, M. Mirov, S. Vasilyev, V. Smolski, V. Gapontsev, 140 w cr:znse laser system, *Opt. Express* 24 (2016) 21090–21104.
- [10] I.T. Sorokina, E. Sorokin, Chirped-mirror dispersion controlled femtosecond cr:znse laser, *Advanced Solid-State Photonics*, OSA Technical Digest Series (CD) (Optical Society of America) (2007) WA7.
- [11] M.N. Cizmeciyan, H. Cankaya, A. Kurt, A. Sennaroglu, Operation of femtosecond kerr-lens mode-locked cr:znse lasers with different dispersion compensation methods, *Appl. Phys. B* 106 (2012) 887–892.
- [12] M.N. Cizmeciyan, H. Cankaya, A. Kurt, A. Sennaroglu, Kerr-lens mode-locked femtosecond cr^{2+} :znse laser at 2420 nm, *Opt. Lett.* 34 (2009) 3056–3058.
- [13] Y. Wang, T.T. Fernandez, N. Cocuccelli, A. Gambetta, P. Laporta, G. Galzerano, 47-fs kerr-lens mode-locked cr:znse laser with high spectral purity, *Opt. Express* 25 (2017) 25193–25200.
- [14] N. Nagl, S. Gröbmeyer, V. Pervak, F. Krausz, O. Pronin, K.F. Mak, Directly diode-pumped, kerr-lens mode-locked, few-cycle cr:znse oscillator, *Opt. Express* 27 (2019) 24445–24454.
- [15] S. Vasilyev, M. Mirov, V. Gapontsev, High power kerr-lens mode-locked femtosecond mid-ir laser with efficient second harmonic generation in

- polycrystalline $\text{Cr}^{2+}:\text{ZnS}$ and $\text{Cr}^{2+}:\text{ZnSe}$, *Advanced Solid State Lasers*, OSA Technical Digest (Optical Society of America) (2014) AM3A.3.
- [16] S.O. Leonov, Y. Wang, V.S. Shiryaev, G.E. Snopatin, B.S. Stepanov, V. G. Plotnichenko, E. Vicentini, A. Gambetta, N. Coluccelli, C. Svelto, P. Laporta, G. Galzerano, Coherent mid-infrared supercontinuum generation in tapered suspended-core $\text{As}_{39}\text{Se}_{61}$ fibers pumped by a few-optical-cycle $\text{Cr}:\text{ZnSe}$ laser, *Opt. Lett.* 45 (2020) 1346–1349.
- [17] S. Vasilyev, I. Moskalev, M. Mirov, S. Mirov, V. Gapontsev, Three optical cycle mid-ir Kerr-lens mode-locked polycrystalline $\text{Cr}^{2+}:\text{ZnS}$ laser, *Opt. Lett.* 40 (2015) 5054–5057.
- [18] S. Vasilyev, I. Moskalev, V. Smolski, J. Peppers, M. Mirov, Y. Barnakov, V. Fedorov, D. Martyshkin, S. Mirov, V. Gapontsev, Kerr-lens mode-locked $\text{Cr}:\text{ZnS}$ oscillator reaches the spectral span of an optical octave, *Opt. Express* 29 (2021) 2458–2465.
- [19] T.J. Carrig, G.J. Wagner, A. Sennaroglu, J.Y. Jeong, C.R. Pollock, Mode-locked $\text{Cr}^{2+}:\text{ZnSe}$ laser, *Opt. Lett.* 25 (2000) 168–170.
- [20] I.T. Sorokina, E. Sorokin, Femtosecond pulse generation from a sesam mode-locked $\text{Cr}:\text{ZnSe}$ laser, *Conference on Lasers and Electro-Optics/Quantum Electronics and Laser Science Conference and Photonic Applications Systems Technologies*, Technical Digest (CD) (Optical Society of America) (2006) CMQ2.
- [21] M.N. Cizmeciyan, J.W. Kim, S. Bae, B.H. Hong, F. Rotermund, A. Sennaroglu, Graphene mode-locked femtosecond $\text{Cr}:\text{ZnSe}$ laser at 2500 nm, *Opt. Lett.* 38 (2013) 341–343.
- [22] R.W. Stites, S.A. McDaniel, J.O. Barnes, D.M. Krein, J.H. Goldsmith, S. Guha, G. Cook, Hot isostatic pressing of transition metal ions into chalcogenide laser host crystals, *Opt. Mat. Express* 6 (2016) 3339–3353.
- [23] J.W. Evans, R.W. Stites, T.R. Harris, Increasing the performance of an $\text{Fe}:\text{ZnSe}$ laser using a hot isostatic press, *Opt. Mat. Express* 7 (2017) 4296–4303.
- [24] T. Brabec, C. Spielmann, P.F. Curley, F. Krausz, Kerr lens mode lockin, *Opt. Lett.* 17 (1992) 1292–1294.
- [25] I.E. Gordon, et al., The hitran2020 molecular spectroscopic database, *J. of Quant. Spect. and Rad. Transfer* 277 (2022) 107949.
- [26] J. Ma, H. Huang, K. Ning, X. Xu, G. Xie, L. Qian, K.P. Loh, D. Tang, Generation of 30-fs pulses from a diode-pumped graphene mode-locked $\text{Yb}:\text{CaYAlO}_4$ laser, *Opt. Lett.* 41 (2016) 890–893.
- [27] M. Mehendale, S. Sivananthan, W.A. Schroeder, Hot electron relaxation dynamics in ZnSe , *Appl. Phys. Lett.* 71 (1997) 1089–1091.
- [28] L. Yan, S. Han, Passive mode locking of inhomogeneously broadened lasers, *J. Opt. Soc. Am. B.* 24 (2007) 2108–2118.